Catalysis Today 168 (2011) 140–146

Contents lists available at ScienceDirect

Catalysis Today

journal homepage: www.elsevier.com/locate/cattod

Platinum clusters confined in FAU–LTA hierarchical porous composite with a core–shell structure

Xiaoqin Zou[a,b], Ka-Lun Wong[a], Sebastien Thomas[a], Till H. Metzger[c,d], Valentin Valtchev[a], Svetlana Mintova[a,*]

[a] Laboratoire Catalyse & Spectrochimie, ENSICAEN – Universite de Caen – CNRS, 6, boulevard du Marechal Juin, 14050 Caen, France
[b] State Key Laboratory of Inorganic Synthesis and Preparative Chemistry, College of Chemistry, Jilin University, Changchun 130012, PR China
[c] European Synchrotron Radiation Facility, ESRF, BP 220, Grenoble 38043, France
[d] Max Planck Institute of Colloids and Interfaces, 14424 Potsdam, Germany

ARTICLE INFO

Article history:
Received 27 September 2010
Received in revised form 6 December 2010
Accepted 7 December 2010
Available online 15 January 2011

Keywords:
Zeolite
Core–shell
Crystal growth
Pt clusters
CO sorption

ABSTRACT

Hierarchical porous composite with a core–shell structure possessing FAU-type zeolite core (zeolite X) and LTA-type zeolite shell (zeolite A) has been prepared. The intimate growth of zeolite shell is achieved by in situ crystallization of the LTA zeolite crystals with size of 1 μm on large single FAU-type crystals with size of about 60–90 μm. Direct visualization of the core–shell material is provided by X-ray microbeam measurements using synchrotron radiation on a single crystal complemented with field emission scanning electron microscopic study. The nitrogen sorption data confirmed that the access to large single FAU-type core is controlled by the defect-free LTA-type shell. Sorption measurements showed that about 98% of core crystals are covered by the LTA shells. Further the FAU–LTA core–shell material is used as a host for the stabilization of platinum clusters. The Pt location, mean size and distribution have been studied by CO chemisorption followed by FT-IR spectroscopy. High loading of platinum accessible to CO molecules in the core–shell material is achieved. The use of the FAU–LTA matrix allowed the stabilization of two different sizes of Pt clusters. Additional advantage of the core–shell material is the protection of the clusters from thermal sintering and poisoning, which is of significant importance for future catalysts.

1. Introduction

The challenge in the field of porous materials is in controlling the size, shape and uniformity of the pores as well as in the fabrication of materials with hierarchical structures [1–5]. The ability to fabricate new multi-porous solids with ordered structures and extraordinary properties makes wider their application beyond the traditional use as catalysts and sorbents. There are a number of strategies available for introducing structural organization into inorganic materials and in the preparation of a hierarchical zeolite material with ordered nano-, meso-, and macroporosity. Besides, a deposition of one type of porous nanoparticles as shell onto another type of porous micrometer-sized crystals to produce nanostructure composites with multimodal porosity is an approach for the creation of hierarchical materials [3–7]. The preparation of porous core–shell materials, where the access to a large core with specific properties is controlled by a tiny shell, with diverse functionalities has attracted considerable attention [5–10]. Special attention has been paid to inorganic porous core–shell materials because of their relatively high thermal, mechanical, and chemical stability [10–13]. Such materials offer certain advantages as chemical sensors, shape selective adsorbents, controlled drug release materials, separation and storage of various species or as catalytic microreactors.

Zeolites are inorganic crystalline aluminosilicates that contain uniform micropores and cavities of molecular dimensions. In the era of nanotechnology, zeolites have also been used to make novel nanostructure synthetic materials, as among them the core–shell zeolite composites take a special place [14–17]. Additionally, great interest has been intrigued if these core–shell zeolite materials are processed as hosts for guest molecules, ions and metal clusters for optical, electric, magnetic and catalytic microdevice applications [18–22]. Besides the aforementioned issues, for catalytic and separation purposes, a material combining one type of zeolite as a core and another continuous zeolite as a shell would show great prospective to meet these requirements and would increase considerably their applications. Very recently, the preparation of core–shell zeolite–zeolite composites possessing core and shell of different structural types was reported. The preparation methods can be categorized mainly into two types, (i) seeded method and (ii) complete epitaxial overgrowth [23–25]. In the first method, pre-

* Corresponding author. Tel.: +33 2 31 45 27 37; fax: +33 2 31 45 28 22.
E-mail address: svetlana.mintova@ensicaen.fr (S. Mintova).

0920-5861/$ – see front matter © 2010 Elsevier B.V. All rights reserved.
doi:10.1016/j.cattod.2010.12.034

liminary adsorption of zeolite nanoseeds on the core crystals and further secondary growth was followed thus allowing for the formation of core–shell zeolite materials. This method applied in the construction of core–shell zeolite materials shows many advantages, such as easily synthesis of many targeted shell on different zeolites and formation of continuous and fully covered shell on zeolite core [23,24]. The concept of epitaxial growth is based on the idea that certain zeolites are composed of identical building units but with different spatial arrangements [25]. Although epitaxial growth often takes place on a specific crystal face and it is restricted to several types of zeolites, the co-crystallization of such materials may lead to intimate intergrowth core–shell structures under specific and elaborated synthesis conditions [26–30]. In the present study we report on the complete overgrowth of zeolite LTA-type shell on FAU-type core by applying the direct growth technique.

Further, supported metal nanoclusters such as Pt, Pd, Ir, Rh, Ru, Au, Ag and Cu within the cavities of zeolites hosts are formed by various techniques and expected to be effective catalysts [31–36]. The placement of clusters within zeolite cages is expected to stabilize the clusters against sintering and poisoning. Platinum is an important and highly active catalyst for the oxidation of CO and residual hydrocarbons in automotive exhaust catalysis and for hydrogenation in petrochemical reactions and other commercial applications [37–39]. However under working conditions, the platinum is unfortunately subjected to deactivation, migration and thus further agglomeration. Consequently, the encapsulation of platinum clusters within well-defined pores of zeolite hosts in order to protect the active structures from agglomeration is highly desired. Having in mind the possible future applications, the core–shell zeolites are envisioned as new host materials for confinement of Pt clusters. On the other hand, the performance of Pt clusters is dependent on their size and degree of homogeneous distribution in the host matrix. Moreover, the behavior of hierarchical Pt nanoclusters confined in the core–shell zeolite is not exploited yet.

Spectroscopy, especially infrared (IR) spectroscopy, is a powerful technique to probe size-dependent behavior of platinum clusters [40–44]. The method provides valuable information on the location, size distribution and dispersion of Pt nanoparticles on the support [45].

The objective of the present study is to develop a convenient route for the preparation of hierarchical porous composite with a core–shell structure combining high adsorption capacity and specific catalytic properties. In order to fulfill the above requirements, FAU–LTA composite with LTA shell and a single FAU core is prepared. The LTA and FAU zeolite topologies are structurally related. Both frameworks include the sodalite cage as a basic building unit. LTA-type and FAU-type frameworks are built by sharing the double 4-rings and 6-rings of the sodalite cage, respectively. Due to the similarities between the two it is anticipated that under specific conditions LTA-type could overgrow the pre-formed FAU crystals. Furthermore, high ion-exchange abilities of FAU–LTA hierarchical porous composite with a core–shell structure make it excellent host for platinum clusters with high loading and high dispersion, which would further serve as an effective catalyst.

2. Experimental

2.1. Reactants

Aluminum powder (99%), triethanolamine (TEA) (99.98%), tetraethylorthosilicate (TEOS) (99.98%), sodium hydroxide (NaOH) (97%), LiCl (97%), sodium silicate (Na_2SiO_3 $9H_2O$) (98%), sodium aluminate ($NaAlO_2$) (98%) (Guangfu Fine Chemical Research Institute, Tianjin, China) and dichlorodiamineplatinum ($Pt(NH_3)_2Cl_2$, 99.9%) (Aldrich) are used as received.

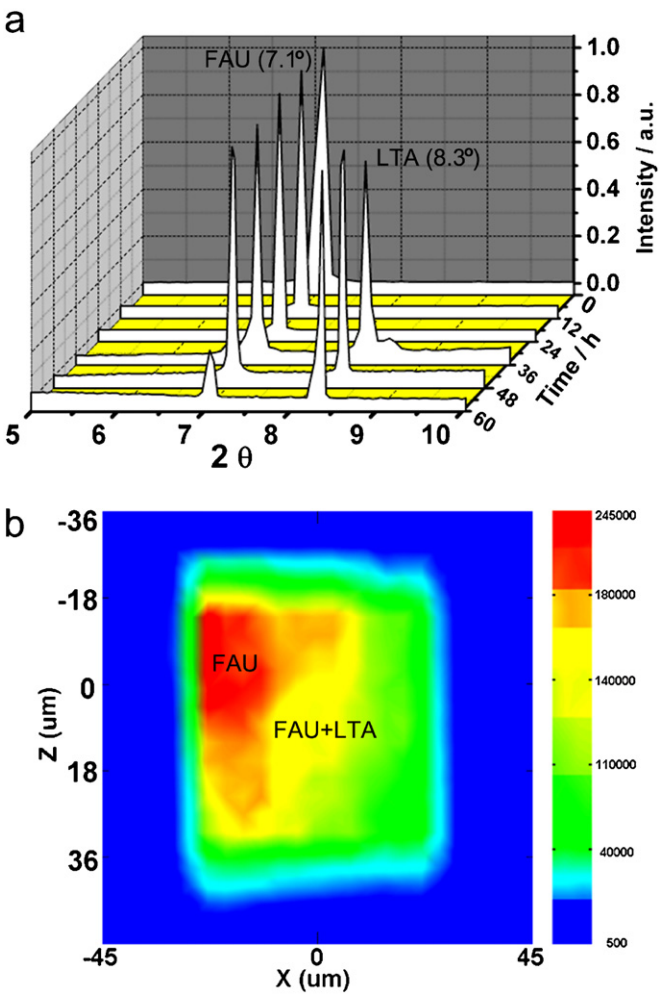

Fig. 1. (a) X-ray diffraction of zeolite X (1 1 1) and zeolite A (2 0 0) peaks of FAU–LTA core–shell material synthesized for: 0 h, 12 h, 24 h, 36 h, 48 h and 60 h; (b) spatially resolved mapping of the micro-beam intensity of (1 1 1) FAU peak (*x* and *z* coordinates define the sample surface, i.e., horizontal and vertical directions, respectively) in the FAU–LTA core–shell composite after 60 h.

2.2. Synthesis of FAU-type zeolite and FAU–LTA hierarchical porous composite with a core–shell structure

Large single FAU-type crystals with a size of 60–90 μm were prepared according to the procedure described in Ref. [46]. Typically, 1.4 g NaOH and 0.21 g aluminum powder were dissolved in 15 ml deionized water and then filtrated to obtain a clear solution (solution 1). The TEOS (1.52 g) and TEA (3.212 g) were dissolved in 15 ml water under stirring for 8 h (solution 2). Then, the two solutions were mixed and stirred for 10 min and transferred into Teflon lined autoclave, which was subjected to heating at 85 °C for 18 days. The synthesized crystals were purified with water until the decanting water reached pH = 8.

Prior to the zeolite A growth the FAU-type crystals were ion-exchanged with 1 M LiCl solution in a single step. The LTA synthesis gel was prepared by mixing 0.55 g $NaAlO_2$ dissolved in 20 ml water and 0.66 g $Na_2SiO_3{\cdot}9H_2O$ dissolved in 20 ml water. The two solutions were mixed under stirring for 10 min. Li-exchanged FAU zeolite crystals were introduced into zeolite A precursor solution ($2.44Na_2O/1.44Al_2O_3/SiO_2/965.2H_2O$) and heated at 85 °C for 12 h, 24 h, 36 h, 48 h, 60 h and 72 h. After the syntheses the FAU–LTA samples were filtrated and dried at room temperature. The core–shell composite and pure FAU zeolite crystals were ion-exchanged with 0.01 M $Pt(NH_3)_2Cl_2$ at 60 °C twice for 12 h. The FAU–LTA core–shell

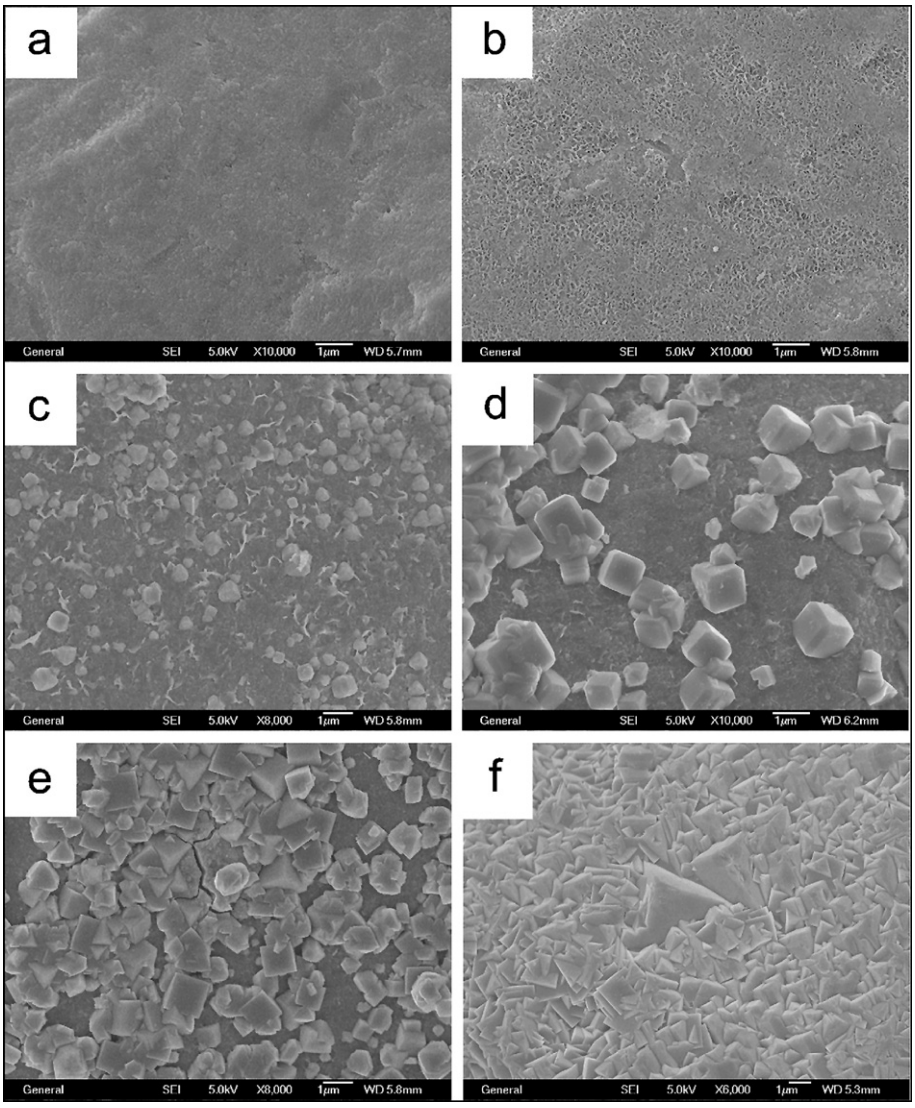

Fig. 2. Surface morphology of FAU single crystals after hydrothermal treatment in zeolite A precursor suspension for (a) 12 h, (b) 24 h, (c) 36 h, (d) 48 h, (e) 60 h, and (f) 72 h recorded with FE-SEM.

composites were separated from the LTA zeolite crystallized in the bulk by ultrasonic treatment and filtration.

2.3. Characterization

FAU–LTA core–shell composite was characterized using a X-ray microbeam (7 keV X-rays, at wavelength of 1.7745 Å) at beamline ID01 at the European Synchrotron Radiation Facility (ESRF) in Grenoble, France. The size of the focused beam (full width half maximum) was 2 μm × 2 μm. A single FAU–LTA crystal was fixed on a silicon wafer with glue. The surface of the sample was tilted by an angle θ close to the (1 1 1) FAU zeolite Bragg reflection ($\theta \approx 3.55^\circ$) and the detector (MAXIPIX: Multichip Assembly for X-ray Imaging based on a photon counting pixel array) was placed at 2θ angle. The sample and detector were aligned so that the diffracted intensity was maximized under the applied conditions.

The powder XRD patterns from the FAU–LTA core–shell composites synthesized after different periods of time were collected using a STOE STADI-P diffractometer equipped with a curved germanium (1 1 1) primary monochromator and a linear position-sensitive detector CuKα1 radiation.

Field-emission scanning electron microscope (FE-SEM: JEOS JSM6700F) was used to characterize the composites prepared for different crystallization times.

Nitrogen adsorption–desorption measurements were carried out on the initial FAU-type zeolite crystals and FAU–LTA core–shell composites using a Micromeritics ASAP 2010 M. Before the measurements, all samples were degassed at 150 °C for 24 h. The specific surface areas of the samples were calculated using Brunauer–Emmet–Teller model from the adsorption branch.

The chemical composition of the samples is measured using a Perkin-Elmer 3030B atomic absorption spectrophotometer. The Si/Al ratios of pure FAU and FAU–LTA core–shell materials are 1.46 and 1.34, respectively.

2.3.1. CO sorption measurements

CO chemisorption experiments have been performed with a static in situ FTIR set-up under vacuum equipped with a cryogenic MCT detector. The Pt-FAU and Pt-FAU–LTA crystals are pressed into self-supporting pellets of 10 mg cm^{-2} suitable for IR measurements in transmission mode. Prior to the measurements, the Pt cations were reduced at 300 °C under hydrogen atmosphere (≈100 Torr);

heating rate of 1 °C/min. Small calibrated doses of CO are sent to the activated samples at room temperature, resulting in an increase of the ν_{CO} IR band corresponding to the CO chemisorbed on Pt. The ν_{CO} bands are integrated in the range 2150–1950 cm^{-1} after each introduction of CO. The amount of Pt accessible to CO has been calculated as described elsewhere [45]. The size and location of Pt clusters was also determined with a transmission electron microscope (TEM). The images were recorded using a JEOL 3010 with an acceleration voltage of 300 kV.

3. Results and discussion

In this study, the synthesis of FAU–LTA core–shell material was performed as follows: firstly, large FAU-type single crystals were freshly prepared in an organic-template-free precursor system according to the procedure described before [46]. As shown in Fig. S1 (see Supporting information), a batch of high-quality single FAU-type crystals with size ranging between 60 and 90 μm with the typical octahedral morphology were obtained. The surface of crystals faces was clean and smooth. Then, the FAU zeolite crystals were subjected to hydrothermal treatment in order to form LTA zeolite shell (see Section 2). The FAU–LTA composite obtained after different synthesis times were characterized by XRD. The evolution of the LTA zeolite shell overgrowing the support crystals (FAU) is shown in Fig. 1, where the change of diffraction peaks in the range of $2\theta = 5–10^\circ$ can be seen. At the beginning of the process, i.e., up to 36 h hydrothermal treatment, the diffracted intensity of (1 1 1) planes of FAU zeolite did not change substantially. After 36 h crystallization, a peak centered at $2\theta = 8.3^\circ$ appears, which is the most intense diffraction (2 0 0) peak of the LTA-type material. The intensity of this peak increased with the prolongation of the synthesis time. The latter is coupled with a decrease in intensity of the peak at $2\theta = 7.1^\circ$, that is, (1 1 1) plane of FAU-type zeolite. A substantial raise in the intensity of the LTA zeolite peak is observed after 60 h crystallization. These observations clearly show that the mass ratio of the two zeolites changed with the extension of crystallization time.

Powdered X-ray diffraction analysis of FAU–LTA composite is complemented with micro-focusing mapping using a synchrotron X-ray facility [47–50]. Fig. 1b represents a map of (1 1 1) peak intensity of FAU-type core crystal over an 80 μm × 80 μm surface. It is worth recalling that the size of the micro-beam is 2 μm × 2 μm, and thus the FAU–LTA core–shell composite is studied with that step of resolution. In the 2D image, the octahedral FAU single crystal appears as a square. The color changes across the single crystal clearly show the intensity differences in diffracted beam and different contributions of FAU-type material (see Fig. 1b). It should be specified, however, that the observed intensity differences are influenced also by crystal morphology and position of diffraction plane. Therefore, to get insights on the formation of LTA zeolite shell, a series of the FAU–LTA composites, representing different stages of shell formation, are studied by FE-SEM (Fig. 2). As can be seen in Fig. 2a, the surface of FAU-type zeolite crystals firstly became rough after 12 h treatment in the highly alkaline LTA precursor suspension (see Supporting information Fig. S1c). It can also be seen that after 24 h crystallization, the surface became rougher (Fig. 2b) due to extended and progressive etching. At this stage, there are many pores and voids on the surface of the FAU-type crystals that might act as nucleation sites for the growth of LTA zeolite crystals. After 36 h crystallization, the first LTA crystals emerge from the rough surface of the support (Fig. 2c). In the beginning of the shell formation, small random crystals can be seen on the surface (Fig. 2d). These crystals continue growing by consuming the nutrients from the mother suspension (Fig. 2e). At the same time new nuclei are formed on the FAU-type zeolite surface. After 72 h crystallization, a continuous shell with no visible pinholes or defects is obtained (Fig. 2f). Thus FAU-type crystal core is completely covered by inter-grown cubic LTA-type crystals with size below 1 μm (Fig. 3a). According to cross section views of the shell layer, the thickness is 1.75 μm (Fig. 3b). Based on the SEM observation one can conclude that the LTA crystallization is preceded by etching the FAU crystal faces, creating high free-energy surfaces that favor the LTA zeolite nucleation. The number of nucleation centers seems to be very high if one considers the extensive intergrowth of crystals forming the shell. Densely packed intergrown LTA zeolite crystals are formed due to steric hindrance and space limitation provoked by the simultaneously growing of numerous nuclei. Summarizing the above results a fairly complete picture of zeolite shell formation can be presented. At the early stage of the crystallization process of the LTA zeolite on the FAU zeolite, a creation of defects on the support surface is observed. The zeolite building units undergo different sequences of rearrangement in these areas and thus provide the nucleation sites for the growth of zeolite A. The growth starts namely from the edge of FAU-type crystals revealing that the edge of crystal face is more vulnerable to dissolution and thus to nucleation in respect to the flat surface in the central part of the (1 1 1) octahedral face. After the initial period of nucleation, the LTA zeolite crystals started to grow thus covering first the edge of the FAU core

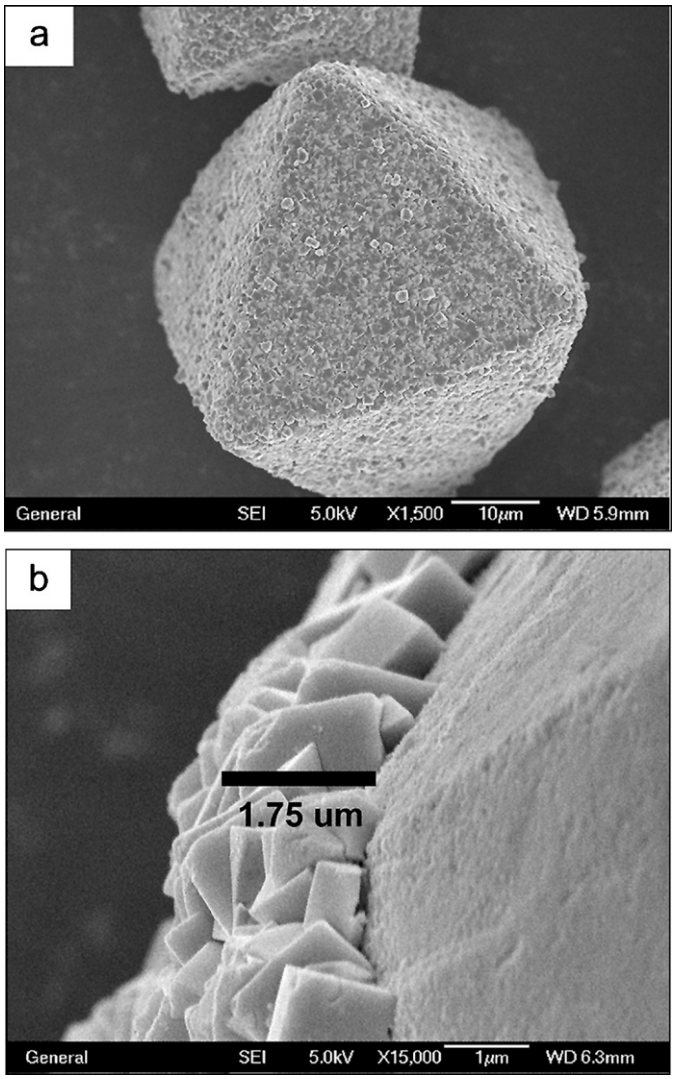

Fig. 3. FE-SEM images of (a) FAU-type core single crystal after synthesis of LTA-type shell for 72 h and (b) cross-sectional view of the interface between LTA-type shell and FAU-type core crystal.

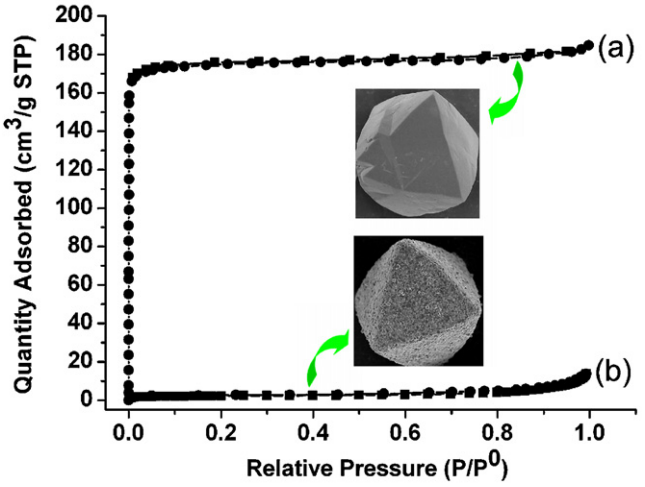

Fig. 4. N_2 adsorption/desorption isotherms of (a) the initial zeolite X single crystals and (b) core–shell FAU–LTA composite. Insets: FE-SEM images of the FAU-type core crystal and the FAU–LTA core–shell material, respectively.

crystals. As the crystallization progress, larger areas in the central part of the FAU zeolite faces are not covered and then completed with time. The increase of the thickness leads to healing the defect parts in the shell as well.

The access to the FAU core *via* the LTA shell is studied by nitrogen sorption measurements. Type I adsorption–desorption isotherm typical for microporous materials, where a steep uptake at low relative pressures is followed by nearly horizontal adsorption and desorption branches, is recorded for pure FAU-type crystals (Fig. 4a). The specific Brunauer–Emmet–Teller surface area (S_{BET}) of zeolite X is 720 $m^2\ g^{-1}$. This value corresponds to a highly crystalline material, which is in a good agreement with the SEM and X-ray diffraction data. The integrity of LTA-type shell is evaluated by N_2 adsorption measurement. As known, the Na-form of zeolite A does adsorb very low amount of N_2 at the temperature of 77 K. Consequently, if the zeolite A shell of core–shell composites does not comprise defects, a material with very low specific surface area should be expected. From the adsorption–desorption isotherm of FAU–LTA core–shell material, a low S_{BET} of 7.8 $m^2\ g^{-1}$ is determined (Fig. 4b). The latter unambiguously shows that the intergrown LTA shell controlled the access to FAU-type core.

As mentioned in the introduction section, small platinum clusters dispersed in zeolite cavities are largely used in heterogeneous catalysis. In general, the platinum metal species diffuse and migrate from nearby sites and form bigger Pt clusters under hydrogen reduction, especially in a highly loaded host. Therefore, it is important to study particularities of Pt clusters in the FAU–LTA core–shell composite, and compare with their counterparts in the pure FAU-type crystals. HRTEM images of Pt clusters in FAU–LTA core–shell composite in the initial FAU-type crystals are shown in Fig. 5a and b. Two classes of Pt particles are observed in the core–shell material (Fig. 5a), while homogeneous in size clusters are found in the FAU-type zeolite (Fig. 5b). FAU–LTA core–shell composite comprised Pt particles with diameter in the range of 1–3 nm and 3–5 nm, while only the latter is present in the initial FAU-type material.

Further, CO chemisorption was used to shed light on the Pt dispersion and location in the FAU zeolite and FAU–LTA core–shell materials. In both samples, the Pt is introduced twice and reduction under hydrogen is carried out followed by CO chemisorption with different doses. Fig. 6a and b shows the IR spectra of CO chemisorbed on the Pt clusters in pure FAU-type and FAU–LTA core–shell samples, respectively. For pure FAU-type sample, the shape of the IR band does not change significantly under the addition of small doses of CO, thus indicating a uniform particle size and location of the Pt clusters. In the case of FAU–LTA core–shell composite the relative contributions from the CO at low and high wavenumbers vary with increasing the dose of CO that pointed out the presence of two distinct platinum species. The set of spectra recorded for FAU–LTA core–shell material is further analyzed using the MCR-ALS method [51]. The MCR-ALS method allows the decomposition of the IR spectra, thus the evolution of CO adsorbed on Pt particles with different sizes and/or location can be discriminated [45]. Here, a decomposition corresponding to two types of Pt species is chosen since the platinum is expected to be in the core and in the shell. The results from this analysis are depicted in Fig. 6c and d. The spectrum with a band having a maximum at 2070 cm^{-1} (Fig. 6c1) is attributed to CO adsorbed on the platinum located in

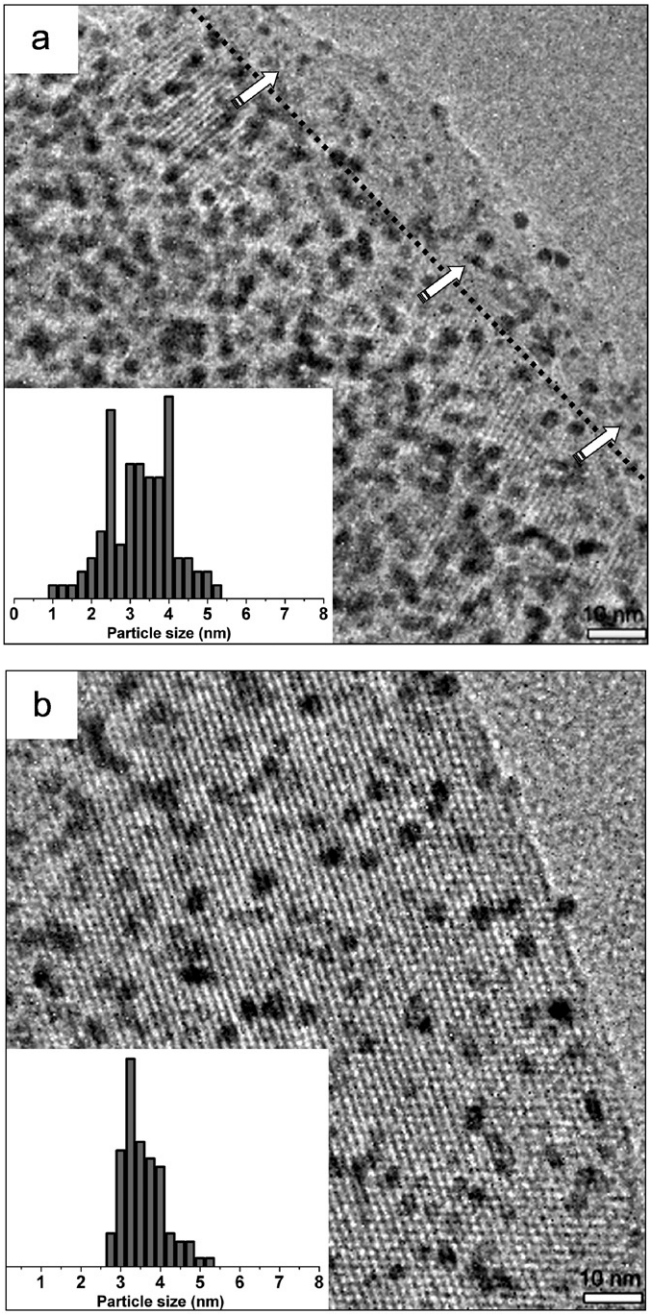

Fig. 5. TEM images of Pt in (a) FAU–LTA core–shell and (b) FAU-type crystals. Insets: particle size distribution of Pt. Dashed line: border line between FAU core and LTA shell.

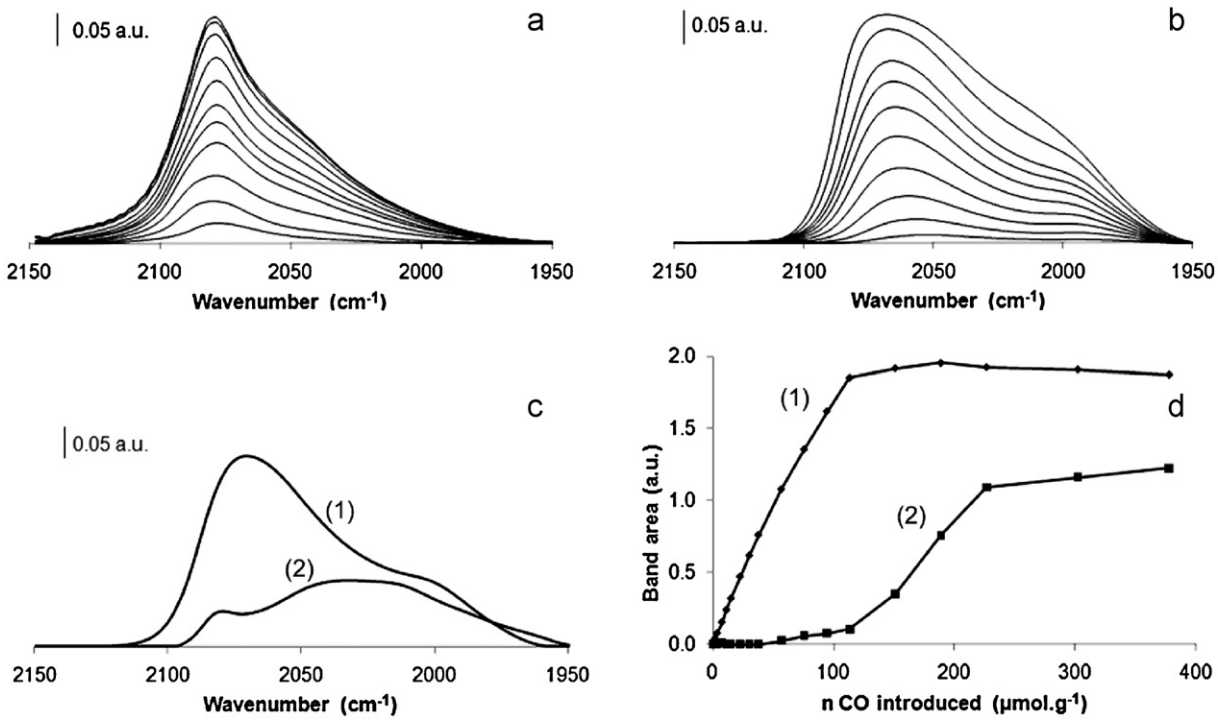

Fig. 6. IR spectra of CO adsorbed with different amounts on Pt in (a) pure FAU-type material and (b) FAU–LTA core–shell composite. MCR-ALS spectra calculated for CO chemisorbed on (1) big and (2) small Pt particles in the FAU–LTA core–shell sample at (c) saturation and (d) evolution of the relative contributions from (1) big and (2) small Pt particles at low CO doses.

Table 1
Properties of Pt clusters in the FAU–LTA core–shell and pure FAU-type material determined from CO chemisorption IR study, chemical analysis and TEM measurements.

Sample	Loading[a] (wt.%)	Dispersion[b] (%)	Particle size			
			CO chemisorption		TEM	
			d_{small} (nm)	d_{big} (nm)	d_{small} (nm)	d_{big} (nm)
FAU–LTA	17.0	29.0	2.5	6.3[c]	2.3	3.7
FAU	11.6	15.1	6.3		3.6	

[a] Chemical analysis.
[b] CO IR analysis.
[c] Under assumption to be equal to the particle size in the FAU sample.

the core, and similar spectra are recorded for the pure FAU-type sample (Fig. 6a). At lower wavenumber at 2040 cm^{-1}, the band is attributed to the CO adsorbed on platinum in the shell (Fig. 6c2).

Additional information about the size of the Pt clusters is extracted from the shape of two spectra. As known, big particles exhibit higher coordinated surface atoms (planes) than the small ones for which the proportion of the edges and corners is higher. As a consequence, the CO molecules are adsorbed on the small particles leading to consequent appearance of the IR bands, first at lower wavenumbers (platinum particles located in the shell), then at higher wavenumbers (platinum particles located in the core) [41,52]. This finding is in a good agreement with the two sizes of Pt clusters observed by TEM in the core–shell sample (Table 1).

Based on the CO adsorption on Pt in FAU–LTA core–shell and pure FAU-type samples, the degree of dispersion and the particle size of the clusters are calculated (Table 1). For the FAU–LTA core–shell sample, local loading and dispersion of platinum in the core are evaluated to be in the range of pure FAU-type sample. It is worth mentioning that both samples are rich of Pt which is expected for the materials exhibiting high ion-exchange capacities. In the FAU–LTA core–shell and pure FAU-type crystals the amount of Pt loaded is 17.0% and 11.6%, respectively. The two samples differed also in the degree of dispersion, i.e., is 29% and 15%, respectively. This can be explained by the presence of two types of zeolites with high ion-exchange capacity. The Si/Al ratio of pure FAU-type and FAU–LTA composite is 1.46 and 1.34, justifying the high Pt loading. On the other hand, the Si/Al ratio of 1.02 of zeolite A crystals is in a good agreement with both high loading and level of dispersion in the core–shell material. These results revealed also that the Pt clusters in FAU-type material are fused forming bigger entities (see Table 1). The location of small Pt clusters in LTA-type zeolite and large Pt in FAU-type zeolite is also confirmed by TEM and CO study using IR. Thus, due to the bi-modal pore system of core–shell material, two different classes of Pt clusters highly accessible to CO are stabilized. Although the size of cavities in FAU and LTA types zeolites is similar, the pore openings are different, which is the most plausible reason for the observed different Pt clusters.

4. Conclusions

The preparation of Pt functionalized hierarchical porous composite with a core–shell structure was studied. The preparation procedure involves: (i) synthesis of large single FAU-type crystals, which were further used as core of the composite; (ii) growth of LTA-type continuous shell on FAU-type core; and (iii) incorporation of Pt clusters *via* ion-exchange and reduction in hydrogen atmo-

sphere under vacuum. The mechanism of the overgrowth process was studied by FE-SEM and X-ray microbeam measurements using synchrotron radiation. The first stage of shell formation involves etching and creation of active sites on FAU-type zeolite crystals faces. These highly active zones induced zeolite A crystallization. A propagation of zeolite shell from zeolite X crystal edges to the central part of the faces was observed until complet coverage of the core crystal. The integrity of the LTA-type shell and the control access to the FAU-type core was demonstrated by N_2 adsorption measurements.

The hierarchical porous composite with a core–shell structure was found appropriate for hosting platinum clusters with high accessibility and stability which was demonstrated by in situ CO chemisorption followed by FT-IR spectroscopy. The core–shell composite offered the advantage of the formation of Pt clusters with different sizes and levels of dispersion. Thus the catalytic performance of a catalyst could finely be tuned by employing such complex materials.

Acknowledgement

The authors gratefully acknowledge funding from the SRIF PNANO ANR Project.

Appendix A. Supplementary data

Supplementary data associated with this article can be found, in the online version, at doi:10.1016/j.cattod.2010.12.034.

References

[1] J. Pérez-Ramírez, C.H. Christensen, K. Egeblad, C.H. Christensen, J.C. Groen, Chem. Soc. Rev. 37 (2008) 2530.
[2] J. Pérez-Ramírez, D. Verboekend, A. Bonilla, S. Abelló, Adv. Funct. Mater. 19 (2009) 3972.
[3] V.N. Shetti, J. Kim, R. Srivastava, M. Choi, R. Ryoo, J. Catal. 254 (2008) 296.
[4] G. Maduraiveeran, R. Ramaraj, Anal. Chem. 81 (2009) 7552.
[5] H.C. Xin, J. Zhao, S.T. Xu, J.P. Li, W.P. Zhang, X.W. Guo, E.J.M. Hensen, Q.H. Yang, C. Li, J. Phys. Chem. C 114 (2010) 6553.
[6] J. Zhou, Z.L. Hua, X.Z. Cui, Z.Q. Ye, F.M. Cui, J.L. Shi, Chem. Commun. 46 (2010) 4994.
[7] Y.J. Wang, F. Caruso, Adv. Funct. Mater. 14 (2004) 1012.
[8] D.J. Wang, G.B. Zhu, Y.H. Zhang, W.L. Yang, B.Y. Wu, Y. Tang, Z.K. Xie, New J. Chem. 29 (2005) 272.
[9] N. Navascués, C. Téllez, J. Coronas, Micropor. Mesopor. Mater. 112 (2008) 561.
[10] S.B. Yoon, K. Sohn, J.Y. Kim, C.H. Shin, J.S. Yu, T. Hyeon, Adv. Mater. 14 (2002) 19.
[11] E.A. Khan, E.P. Hu, Z.P. Lai, Micropor. Mesopor. Mater. 118 (2009) 210.
[12] Y.J. Chen, P. Gao, C.L. Zhu, R.X. Wang, L.J. Wang, M.S. Cao, X.Y. Fang, J. Appl. Phys. 106 (2009) 054303.
[13] Y.J. Chen, P. Gao, R.X. Wang, C.L. Zhu, L.J. Wang, M.S. Cao, H.B. Jin, J. Phys. Chem. C 113 (2009) 10061.
[14] A.G. Dong, N. Ren, W.L. Yang, Y.J. Wang, Y.H. Zhang, D.J. Wang, H.H. Hu, Z. Gao, Y. Tang, Adv. Funct. Mater. 13 (2003) 943.
[15] J.S. Yu, S.B. Yoon, Y.J. Lee, K.B. Yoon, J. Phys. Chem. B 109 (2005) 7040.
[16] D.J. Kong, J.L. Zheng, X.H. Yuan, Y.D. Wang, D.Y. Fang, Micropor. Mesopor. Mater. 119 (2009) 91.
[17] Y. Fan, D. Lei, G. Shi, X.J. Bao, Catal. Today 114 (2006) 388.
[18] T. Doussineau, M. Smaïhi, G.J. Mohr, Adv. Funct. Mater. 19 (2009) 117.
[19] Y.H. Deng, C.H. Deng, D.W. Qi, C. Liu, J. Liu, X.M. Zhang, D.Y. Zhao, Adv. Mater. 21 (2009) 1377.
[20] A. Corma, U. Díaz, B. Ferrer, V. Fornés, M.S. Galletero, H. García, Chem. Mater. 16 (2004) 1170.
[21] M. Moghadam, S. Tangestaninejad, V. Mirkhani, I. Mohammadpoor-Baltork, M. Moosavifar, J. Mol. Catal. A: Chem. 302 (2009) 68.
[22] K.L. Wong, A. Souici, V.D. Waele, M. Mostafavi, T.H. Metzger, S. Mintova, Langmuir 26 (2010) 4459.
[23] Y. Bouizi, I. Diaz, L. Rouleau, V.P. Valtchev, Adv. Funct. Mater. 15 (2005) 1955.
[24] Y. Bouizi, L. Rouleau, V.P. Valtchev, Chem. Mater. 18 (2006) 4959.
[25] http://www.iza-online.org.
[26] M.S. Francesconi, Z.E. Lopez, D. Uzcategui, G. González, J.C. Hernández, A. Uzcátegui, A. Loaiza, F.E. Imbert, Catal. Today 107–108 (2005) 809.
[27] A.M. Goossens, B.H. Wouters, V. Buschmann, J.A. Martens, Adv. Mater. 11 (1999) 561.
[28] T. Wakihara, S. Yamakita, K. Iezumi, T. Okubo, J. Am. Chem. Soc. 125 (2003) 12388.
[29] H.K. Jeong, J. Krohn, K. Sujaoti, M. Tsapatsis, J. Am. Chem. Soc. 124 (2002) 12966.
[30] M. Miyamoto, T. Kamei, N. Nishiyama, Y. Egashira, K. Ueyama, Adv. Mater. 17 (2005) 1985.
[31] W.M.H. Sachtler, Acc. Chem. Res. 26 (1993) 383.
[32] J. Guzman, B.C. Gates, Dalton Trans. (2003) 3303.
[33] H. Yang, H. Chen, J. Chen, O. Omotoso, Z. Ring, J. Catal. 243 (2006) 36.
[34] S. Ohgoshi, I. Nakamura, Y. Wakushima, Stud. Surf. Sci. Catal. 77 (1993) 289.
[35] M. Choi, Z.J. Wu, E. Iglesia, J. Am. Chem. Soc. 132 (2010) 9129.
[36] J. Kecht, Z. Tahri, V.D. Waele, M. Mostafavi, S. Mintova, T. Bein, Chem. Mater. 18 (2006) 3373.
[37] S.I. Matsumoto, Catal. Today 90 (2004) 183.
[38] H.S. Gandhi, G.W. Graham, R.W. McCabe, J. Catal. 216 (2003) 433.
[39] D.E. Webster, Top. Catal. 16 (2001) 33.
[40] B.M. Weckhuysen, Angew. Chem. Int. Ed. 48 (2009) 4910.
[41] P. Bazin, O. Saur, J.C. Lavalley, M. Daturi, G. Blanchard, Phys. Chem. Chem. Phys. 7 (2005) 187.
[42] K. Chakarova, M. Mihaylov, K. Hadjiivanov, Catal. Commun. 6 (2005) 466.
[43] P. Kubanek, H.W. Schmidt, B. Spliethoff, F. Schuth, Micropor. Mesopor. Mater. 77 (2005) 89.
[44] A.Y. Stakheev, E.S. Shpiro, O.P. Tkachenko, N.I. Jaeger, G. Schulz-Ekloff, J. Catal. 169 (1997) 382.
[45] V. Perrichon, L. Retailleau, P. Bazin, M. Daturi, J.C. Lavalley, Appl. Catal. A 260 (2004) 1.
[46] S. Qiu, J. Yu, G. Zhu, O. Tesaraki, Y. Nozue, W. Pang, R. Xu, Micropor. Mesopor. Mater. 21 (1998) 245.
[47] B. Krause, C. Mocuta, T.H. Metzger, Phys. Rev. Lett. 96 (2006) 165502.
[48] C.E. Murray, M. Sankarapandian, Appl. Phys. Lett. 90 (2007) 171919.
[49] C. Mocuta, J. Stangl, K. Mundboth, T.H. Metzger, G. Bauer, I.A. Vartanyants, M. Schmidbauer, T. Boeck, Phys. Rev. B 77 (2008) 245425.
[50] S.M. Polvino, C.E. Murray, Ö. Kalenci, I.C. Noyan, B. Lai, Z.H. Cai, Appl. Phys. Lett. 92 (2008) 224105.
[51] J. Saurina, R. Tauler, Analyst 125 (2000) 2038.
[52] R.M. Rioux, J.D. Hoefelmeyer, M. Grass, H. Song, K. Niesz, P.D. Yang, G.A. Somorjai, Langmuir 24 (2008) 198.